

1 **CARM1 regulates senescence during airway epithelial cell injury in COPD pathogenesis**

2

3 Rim S. J. Sarker<sup>1\*</sup>, Thomas M. Conlon<sup>1\*</sup>, Carmela Morrone<sup>1</sup>, Barkha Srivastava<sup>1</sup>, Nur Konyalilar<sup>2</sup>,  
4 Stijn E. Verleden<sup>3</sup>, Hasan Bayram<sup>2</sup>, Heinz Fehrenbach<sup>4</sup>, Ali Önder Yildirim<sup>1</sup>

5 1. Comprehensive Pneumology Center (CPC), Institute of Lung Biology and Disease, Helmholtz  
6 Zentrum München, Munich, Germany, Member of the German Center for Lung Research (DZL)

7 2. Koç University Research Center for Translational Medicine (KUTTAM), School of Medicine, Koç  
8 University, Istanbul, Turkey

9 3. Division of Pneumology, KU Leuven, Leuven, Belgium

10 4. Research Center Borstel, Leibniz Lung Center, Experimental Pneumology, Airway Research  
11 Center North (ARCN), Borstel, Germany, Member of the German Center for Lung Research  
12 (DZL)

13

14 \* Contributed equally

15

16 **Author Contributions:**

17 R.S.J.S., H.F. and A.Ö.Y. conceived the study and experimental design. R.S.J.S., C.M., B.S. and NK  
18 performed experiments. SEV prepared patient lung core samples. R.S.J.S., C.M., B.S., H.B., T.M.C. and  
19 A.Ö.Y. analyzed and interpreted the data. R.S.J.S., T.M.C. and A.Ö.Y. wrote the manuscript. All authors  
20 read and edited the manuscript.

21

22 **Running Head:**

23 CARM1 regulates airway epithelial senescence

24

25 **Address for Correspondence:**

26 Ali Önder Yildirim

27 Comprehensive Pneumology Center, Institute of Lung Biology and Disease, Helmholtz Zentrum

28 München, Ingolstädter Landstraße 1, 85764 Neuherberg, Germany

29 [oender.yildirim@helmholtz-muenchen.de](mailto:oender.yildirim@helmholtz-muenchen.de)

30 **Abstract**

31 Chronic obstructive pulmonary disease (COPD) is a life-threatening lung disease. Although cigarette  
32 smoke was considered the main cause of development, the heterogeneous nature of the disease leaves  
33 it unclear whether other factors contribute to the predisposition or impaired regeneration response  
34 observed. Recently, epigenetic modification has emerged to be a key player in the pathogenesis of  
35 COPD. The addition of methyl groups to arginine residues in both histone and non-histone proteins by  
36 protein arginine methyltransferases (PRMTs), is an important posttranslational epigenetic modification  
37 event regulating cellular proliferation, differentiation, apoptosis and senescence. Here, we hypothesize  
38 that coactivator-associated arginine methyltransferase-1 (CARM1) regulates airway epithelial cell injury  
39 in COPD pathogenesis by controlling cellular senescence. Using the naphthalene (NA)-induced mouse  
40 model of airway epithelial damage, we demonstrate that loss of CC10-positive club cells is accompanied  
41 by a reduction in CARM1 expressing cells of the airway epithelium. Furthermore, *Carm1*  
42 haploinsufficient mice showed perturbed club cell regeneration following NA-treatment. In addition,  
43 CARM1 reduction led to decreased numbers of anti-senescent sirtuin 1-expressing cells accompanied by  
44 higher p21, p16 and beta-galactosidase-positive senescent cells in the mouse airway following NA-  
45 treatment. Importantly, CARM1-silenced human bronchial epithelial cells showed impaired wound  
46 healing and higher beta-galactosidase activity. These results demonstrate that CARM1 contributes to  
47 airway repair and regeneration by regulating airway epithelial cell senescence.

48

49 **Keywords:** airway epithelium, CARM1, COPD, senescence

## 50 **Introduction**

51 Chronic obstructive pulmonary disease (COPD) is a life-threatening lung disease, currently the third  
52 leading cause of death worldwide (28), characterized by chronic bronchitis, small airway remodeling and  
53 emphysema (20, 21, 50). It is a major global health problem and associated with high health-care costs.  
54 The staggering socio-economic burden that comes with COPD treatment is now surpassing any other  
55 disease (29) and thus necessitates a deeper understanding.

56 Airway epithelial cells function as the first host defense barrier against cigarette smoke or  
57 environmental pollutants (18). Club cells are progenitor/stem cells responsible for maintenance of the  
58 airway epithelium following an injury (41). However, extensive epithelial injury may disrupt the  
59 epithelial barrier integrity and cause cell death. Repetitive injury combined with a limited reservoir of  
60 progenitor cells leads to poor regeneration and repair processes resulting in abnormal wound healing.  
61 Contributing greatly to impaired repair processes is airway epithelial cell senescence (37, 52). These  
62 changes in the airway epithelium resulting from injury are early and key events in the development and  
63 progression of COPD (2, 31). Therefore, development of therapeutic strategies against COPD depends on  
64 unraveling the detailed mechanisms of airway injury.

65 Although cigarette smoke remains the greatest risk factor for COPD, epigenetic modification has  
66 recently emerged to be another key player in the pathogenesis of COPD (32, 45, 49). A lesser known  
67 epigenetic regulating event is the post-translational modification of proteins by the addition of methyl  
68 groups to arginine residues by a family of intracellular enzymes termed protein arginine  
69 methyltransferases (PRMTs) (5). Protein arginine methylation is a unique class of protein modification  
70 involved in cellular processes such as cell proliferation, differentiation, apoptosis and senescence (4, 5).  
71 Coactivator-associated arginine methyltransferase 1 (CARM1) or PRMT4 is a key family member. CARM1

72 is known to asymmetrically dimethylate arginine residues of histone H3 and various non-histone  
73 proteins that play essential roles in transcriptional regulation (46, 47), RNA splicing (25, 35) and cellular  
74 senescence (27, 36).

75 A recent analysis of PRMT expression in rat lung, heart, liver and kidney revealed the lung to be a major  
76 source of CARM1, suggesting its possible role in maintaining lung homeostasis (19) . Indeed, CARM1  
77 knockdown resulted in dysregulated proliferation and impaired trans-differentiation of alveolar  
78 epithelial cells (34). Thus, abundant pulmonary expression accompanied by its ability to control cell  
79 proliferation and differentiation make CARM1 a potential target for further investigation in COPD  
80 development and progression. We previously investigated the regulation of CARM1 in the development  
81 and progression of emphysema (44). CARM1 deficiency attenuated SIRT1-regulated anti-senescence,  
82 and thus induced senescence in alveolar epithelial cells resulting in an increased susceptibility to  
83 elastase-induced emphysema (44).

84 Here, we hypothesize that CARM1 also regulates airway epithelial cell injury by controlling cellular  
85 senescence. As club cells are crucial to the homeostasis of distal airways in humans (6) and maintain the  
86 airway following injury (41), we took advantage of the established mouse model of club cell targeted  
87 naphthalene (NA)-induced airway epithelial damage (40, 51). We demonstrated that CARM1 expression  
88 was downregulated in NA-treated murine lung accompanied by a loss of CC10-positive club cells from  
89 the airways. *Carm1*<sup>+/-</sup> mice demonstrated impaired club cell regeneration following NA treatment  
90 accompanied by enhanced levels of senescent airway epithelial cells. Moreover, CARM1-silenced human  
91 bronchial epithelial (HBE) cells showed aberrant wound healing and significantly higher levels of beta-  
92 galactosidase-positive senescent cells. Taken together, these findings suggested that CARM1 is  
93 indispensable for airway epithelial regeneration and repair in murine lung by acting as a crucial regulator

94 of cellular senescence. We propose that the findings obtained from this study could help develop novel  
95 therapeutic strategies to target the airway destruction observed in COPD.

96

97 **Materials and Methods**

98 *Human Lungs*

99 Explant lungs were collected in KU Leuven, Leuven Belgium following ethical approval by Institutional  
100 Review Board (S52174). These lungs were considered unsuitable for transplantation due to a variety of  
101 reasons (kidney tumor, microthrombi and logistics), but were histologically normal. Declined donor  
102 lungs can be used for research after second opinion examination under existing Belgian law. After  
103 excision, lungs were air inflated at 10cm water pressure and fixed under liquid nitrogen vapor, before  
104 being sliced into 2cm slices with a band saw and sampled with a core bore (diameter 1.4cm). Lung cores  
105 were sliced, fixed in 6% paraformaldehyde, embedded in paraffin and cut into 3  $\mu$ m sections.

106

107 *Study Patients and Bronchial Tissue.*

108 Lung explants were obtained from 8 patients (all males), who were smokers and had COPD at stage 2  
109 according to the guidelines for the global initiative for obstructive lung disease (1) and from 10 patients  
110 (4 females, 6 males), who were smokers but had no obstructive pulmonary disease. Patient's  
111 characteristics are summarized in Table 1. Before entering the study, the patients were clinically stable  
112 and had received no systemic antibiotics, steroids, cytostatic medications or radiotherapy. Patients were  
113 administered short-acting beta-2 agonists or anti-cholinergic treatments, as needed. None of the study  
114 subjects had upper or lower airway infections within the first month of the study. The study was  
115 approved by The Ethics Committee of Koc University, and informed written consents were taken from  
116 study volunteers. Bronchial tissue obtained from lung explants from patients, who had lobectomy or  
117 pneumonectomy for lung cancer or other reasons at Koc University, Research and Training Hospital  
118 (Turkey). The tissue confirmed as "normal" and macroscopically tumor free by a pathologist was

119 transferred to the molecular biology laboratory. The explant was stored at -80°C until being processed  
120 for qPCR studies. RNA was isolated using RNeasy kit (Qiagen).

121

### 122 *Experimental animals*

123 Pathogen-free female C57BL/6N mice aged between eight and ten weeks of age were purchased from  
124 Charles River Laboratories (Sulzfeld, Germany). The *Carm1*<sup>+/-</sup> mice were generously provided by Prof  
125 Mark Bedford (MD Anderson Cancer Center, University of Texas, Houston, TX) and maintained on a  
126 C57BL/6N background. Mice were housed in chambers maintained at constant temperature and  
127 humidity with a 12-hour light cycle and were allowed to access rodent laboratory chow and water ad  
128 libitum. All animal experiments were performed following strict governmental and international  
129 guidelines. The protocol was approved by the ethics committee of the regional Government for Upper  
130 Bavaria.

131

### 132 *Experimental Protocols*

133 C57BL/6N mice and *Carm1*<sup>+/-</sup> mice were intra-peritoneally injected once with 200mg/kg body weight of  
134 Naphthalene (NA) (Sigma, Munich, Germany) dissolved in Mazola corn oil (CO). Control mice received  
135 only CO. Wild type (WT) mice were analyzed on day 3, 7, 14 and 28 while CARM1 heterozygous animals  
136 were analyzed on day 14. Body weights of mice were taken at each time point. All mice weighed  
137 between 21-26g and were between 10-14 weeks of age at the time of administration. Mice were  
138 anaesthetized with intra-peritoneal injection of ketamine and xylazine, tracheostomized for



139 bronchoalveolar lavage collection and sacrificed by terminal exsanguination on the day of analysis.

140 Experiments were repeated twice (n= 4-7/group in each experiment).

141

#### 142 *Bronchoalveolar lavage (BAL) collection*

143 The lungs were lavaged by instilling with 3 x 0.5 ml aliquots of sterile PBS containing protease inhibitor

144 (Roche). Cells were spun down at 400 g and total cell counts were determined in a hemocytometer via

145 Trypan Blue exclusion method. Differential cell counts (200 cells/sample) were performed using

146 morphological criteria following Giemsa staining (Merck, Darmstadt, Germany).

147

#### 148 *Lung processing and histology*

149 Right lungs were snap frozen in liquid nitrogen, homogenized and total RNA isolated (peqGOLD Total

150 RNA Kit, Peqlab, Erlangen, Germany) for gene expression analysis. The left lung was fixed at 20 cm H<sub>2</sub>O

151 pressure with 6% paraformaldehyde (PFA). Following an overnight fixation in PFA, the tissue was

152 dehydrated, paraffin-embedded and cut in 3 µm sections. Tissues were stained with Hematoxylin and

153 Eosin (H&E) (Merck, Darmstadt, Germany). High resolution histological images were taken using MIRAX

154 Desk (Zeiss, Oberkochen, Germany) and were analyzed using Mirax Viewer software (Zeiss).

155

#### 156 *Immunohistochemistry*

157 The paraffin embedded lung sections were de-paraffinized in xylene and rehydrated. The tissue was

158 treated with 1.8% (v/v) H<sub>2</sub>O<sub>2</sub> solution (Sigma, St. Louis, MO) for 20 minutes to block endogenous

159 peroxidase activity. Heat induced epitope retrieval (30 min at 125 °C; 10 min at 90 °C) was performed in  
160 HIER Citrate Buffer (pH 6.0, Zytomed Systems, Berlin, Germany) in a Decloaking chamber (Biocare  
161 Medical, Concord, CA). Nonspecific binding was inhibited with a blocking antibody (Biocare Medical).  
162 Tissue sections were incubated overnight at 4°C with primary antibodies against CC10 (1:1000, ab40873,  
163 Abcam, Cambridge, UK), CARM1 (1:250, ab87910, Abcam), SIRT1 (1:50, 07-131, Millipore, Darmstadt,  
164 Germany), p21 (1:200, sc-397, Santa Cruz, Dallas, TX), p16 (1:50, sc-1207, Santa Cruz) or beta  
165 galactosidase (1:250, A11132, ThermoFisher Scientific, Waltham, MA) followed by incubation with an  
166 alkaline phosphatase-labeled secondary antibody (Biocare Medical) for 1 hour at room temperature.  
167 Signals were amplified by a chromogen substrate Vulcan fast red (Biocare Medical). Tissues were  
168 counterstained with hematoxylin (Sigma), dehydrated in xylene and mounted with Entellan (Merck  
169 Millipore, Billerica, MA).

170

### 171 *Immunofluorescence*

172 De-paraffinized lung sections were rehydrated, heat-induced epitope retrieval was undertaken using  
173 HIER Citrate Buffer (pH 6.0, Zytomed Systems, Berlin, Germany) and blocked with 5% BSA in PBS for 30  
174 min. Then the lung sections were incubated overnight at 4°C with primary antibodies against CC10  
175 (1:2000, ab40873, Abcam, Cambridge, UK),  $\beta$ -tubulin (1:100, sc-5274, Santa Cruz Biotechnology,  
176 Heidelberg, Germany), keratin14 (1:50, ab7800, Abcam), SIRT1 (1:100, 07-131, Merck, Darmstadt,  
177 Germany) or beta-galactosidase (1:100, A-11132, Invitrogen, Thermo Fisher Scientific, Waltham, MA),  
178 followed by 1 hour incubation with goat anti-rabbit IgG Alexa Fluor 568 labeled secondary antibody  
179 (1:250, Invitrogen), goat anti-rabbit IgG Alexa Fluor 555 labeled secondary antibody (1:500, Invitrogen)  
180 or goat anti-mouse IgG Alexa Fluor 488 labeled secondary antibody (1:500, Invitrogen). To detect

181 CARM1 on the same section, the lung slices were washed in PBS and again blocked with 5% BSA. Next,  
182 the slices were incubated overnight at 4°C with a primary antibody against CARM1 (1:100, ab87910,  
183 Abcam) followed by 1 hour incubation with donkey anti-rabbit IgG Alexa Fluor 488 labeled secondary  
184 antibody (1:250, Invitrogen) or goat anti-rabbit IgG Alexa Fluor 555 labeled secondary antibody (1:500,  
185 Invitrogen) and with 4',6-diamidino-2-phenylindole (DAPI 1:2000, Sigma, St.Louis, MO) for nuclear  
186 counterstaining. Sections were mounted in fluorescent mounting medium (Dako, Agilent, Santa Clara,  
187 CA) and imaged with a fluorescent Olympus BX51 microscope running cellSens software (Version 1.14,  
188 Build 14116, Olympus, Hamburg, Germany).

189

#### 190 *Quantitative Morphometry*

191 Airway epithelial cells positive for CC10, CARM1, SIRT1, p16, p21 or beta galactosidase were quantified  
192 by design-based stereology using a physical dissector. The stereology system consisted of an Olympus  
193 BX51 light microscope equipped with the new Computer Assisted Stereological Toolbox (newCAST)  
194 software (Visiopharm, Hoersholm, Denmark). The number of positively stained cells was determined as  
195 a percentage of the total number of cells positioned on the basal membrane of the airways.

196

#### 197 *Quantitative Real Time PCR*

198 Reverse transcribed cDNA was synthesized using Random Hexamers and Reverse Transcriptase (Applied  
199 Biosystems, Darmstadt, Germany) from right lung isolated total RNA. cDNA was amplified with Platinum  
200 SYBR Green qPCR SuperMix (Applied Biosystems) on a StepOnePlus™ PCR System (Applied Biosystems)

201 using *Hprt1* as a reference gene. Primers are listed in Table 2. Relative gene expression presented as  $2^{-\Delta\Delta Ct}$   
202 ( $\Delta Ct = Ct_{\text{target}} - Ct_{\text{reference}}$ ) and relative change to control as  $2^{-\Delta\Delta Ct}$  ( $\Delta\Delta Ct = \Delta Ct_{\text{treated}} - \Delta Ct_{\text{control}}$ ).

203

#### 204 *Western Blot Analysis*

205 Protein concentrations were determined using the Pierce BCA Protein Assay Kit (Thermo Fisher  
206 Scientific). 20  $\mu\text{g}$  of protein was separated by SDS-PAGE, transferred onto a polyvinylidene difluoride  
207 membrane (Bio-Rad), blocked with 5% non-fat milk and immunoblotted overnight at 4°C with antibodies  
208 against CARM1 (1:1000, Cat. # 09-818, Sigma), asymmetrically dimethylated arginine (ADMA) (1:1000,  
209 Cat. # 07-414, Sigma), SIRT1 (1:1000, Cat. # 84695, Cell Signaling) and p53 (1:1000, Cat. # sc-126, Santa  
210 Cruz Biotechnology). Antibody binding was detected with HRP-conjugated secondary antibodies and  
211 developed using Amersham ECL Prime reagent (GE Healthcare). Bands were detected and quantified  
212 using the Chemidoc XRS system (Bio-Rad), and normalized to  $\beta$ -actin levels (anti- $\beta$ -actin-peroxidase  
213 conjugated mouse monoclonal antibody, AC-15, Cat. # A3854, Sigma).

214

#### 215 *Wound healing assay*

216 Human bronchial epithelial cell line 16HBE (ATCC, Rockville, MD) was seeded at a density of  $4 \times 10^4$  cells  
217 in 24 well plates and transfected 24h later with CARM1-specific siRNAs (Qiagen, Hilden, Germany) using  
218 SuperFect transfection reagent according to manufacturer's instructions (Qiagen) and incubated for 72  
219 hours. Wound healing assay was performed on transfected cells using 200 $\mu\text{l}$  pipette tip to scratch the  
220 cell monolayer. In some experiments siCARM1 cells were additionally treated with 1 $\mu\text{M}$  Resveratrol  
221 (Cat. # R5010, Sigma) 24h before performing the scratch, and un-transfected cells were treated with 25

222 and 50 $\mu$ M Ex-527 (Cat. # E7034, Sigma) for 24h prior to performing the scratch. The size of the wound  
223 was determined at 0 and 18 hours using Axiovision software (Zeiss, Oberkochen, Germany).

224

#### 225 *Senescence-associated beta-galactosidase assay*

226 A staining was performed on CARM1 siRNA transfected 16HBE cells to detect beta galactosidase activity  
227 at pH 6 using a senescence assay kit (Cell signaling, Frankfurt, Germany). Upon fixing the cells with a  
228 solution containing 2% formaldehyde and 0.2% glutaraldehyde in PBS for 10 minutes at room  
229 temperature, the cells were incubated overnight with a staining solution containing 40 mM citric  
230 acid/sodium phosphate (pH 6.0), 150 mM NaCl, 2 mM MgCl<sub>2</sub>, 5 mM potassium ferrocyanide, 5 mM  
231 potassium ferricyanide and 1 mg/ml of X-gal. A percentage of positive cells was determined from 300  
232 cells counted in 12-15 random fields/well.

233

#### 234 *Gene set enrichment analysis (GSEA)*

235 The series matrix file comparing gene expression in the small airway epithelial cells of COPD patients  
236 compared with healthy smoking controls (GSE11784) was downloaded from the NCBI GEO database. To  
237 determine the enrichment of senescence genes (GO: 0090398, obtained from the GSEA-Molecular  
238 Signatures Database), GSEA software from the Broad Institute ([http://www.gsea-  
msigdb.org/gsea/index.jsp](http://www.gsea-<br/>msigdb.org/gsea/index.jsp)) (33, 48) was used.

240

#### 241 *Statistical Analysis*

242 Mean values  $\pm$  S.D. were given unless stated otherwise. Student's un-paired t-test compared two  
243 groups. One-way ANOVA followed by Bonferroni post-test compared more than two groups, if equal  
244 variances and normal distribution was given. Analyses were conducted using GraphPad Prism 6  
245 (GraphPad Software, La Jolla, CA).

246 **Results**

247 **CARM1 expression is downregulated in naphthalene-induced mouse airway injury.**

248 O'Brien et al. previously reported that CARM1 is expressed in alveolar type II (ATII) and club cells in lung  
249 tissue taken from E18.5 mouse embryos (34). Here, we demonstrate that CARM1 is expressed in healthy  
250 adult human airways as well as in adult mouse airways by club cells, indicated by the co-localization of  
251 the club cell marker CC10 and CARM1 following immunofluorescence analysis (Fig. 1A). To further define  
252 the role of CARM1 in airway epithelial cells and its potential contribution to epithelial repair processes,  
253 we took advantage of the NA-induced airway injury mouse model. Previous studies have shown that a  
254 single exposure to NA induces acute and club cell-specific injury in murine airway epithelium (51, 52).  
255 We validated our model by confirming that NA-induced injury, following a single application of  
256 200mg/kg body weight NA i.p., led to a  $73 \pm 1.8\%$  decrease ( $p < 0.001$  vs control) in CC10-positive club  
257 cells at day 3. The airway epithelial injury was followed by gradual club cell regeneration which was  
258 completely resolved by day 28 (Fig. 1B, C). *Scgb1a1* (CC10) expression analysis by quantitative RT-PCR  
259 (qRT-PCR) supported the histological findings of a time-dependent regeneration of club cells in NA-  
260 treated mouse lung (Fig. 1D). Having confirmed the reduction and subsequent regeneration of CC10  
261 positive club cells in the NA injury model, we next investigated CARM1 expression levels during injury.  
262 Quantification of CARM1 positive cells in the airway showed a significant decrease at day 3 ( $58.4 \pm 9.3\%$   
263 NA-treated vs  $83.4 \pm 1.6\%$  controls,  $p < 0.01$ ) following NA application, with the number of CARM1  
264 positive cells restored by day 28 (Fig. 1E, F). Analysis of whole lung homogenate revealed a constant  
265 downregulation of *Carm1* mRNA at all time points following NA injury (Fig. 1G). Taken together, these  
266 data demonstrate that airway injury is associated with a reduction in CARM1 expression in murine  
267 airway epithelial cells and support the idea that CARM1 may be supposed to be involved in airway injury.

268

269 **CARM1 deficiency perturbs club cell regeneration following naphthalene treatment**

270 To further define the function of CARM1 in the airway epithelium, WT and *Carm1*<sup>+/-</sup> mice were exposed  
271 to a single application of NA (200mg/kg i.p.). Mice with a complete knockout of CARM1 cannot survive  
272 beyond late embryogenesis (34). The lungs were examined on day 14 when in wild type (WT) mice club  
273 cell regeneration was ongoing but not yet completed. Fig. 2A clearly demonstrates that the lungs of  
274 *Carm1*<sup>+/-</sup> mice had reduced expression of CARM1 protein compared to WT controls following exposure  
275 to NA, and that this correlated to reduced levels of global asymmetrically dimethylated arginine residues  
276 in lung protein (Fig. 2B). Body weight measurement revealed that NA-treated CARM1 deficient mice  
277 significantly lagged in weight recovery compared to NA-treated WT mice (Fig. 2C). Quantitative  
278 morphometry of CC10-positive club cells demonstrated a significantly reduced percentage of CC10-  
279 positive club cells in *Carm1*<sup>+/-</sup> mouse airway at day 14 compared to WT mice following NA treatment  
280 ( $30.7 \pm 2.5\%$  vs  $62.7 \pm 7.6\%$ ,  $p < 0.01$ ) (Fig. 2D, E). The impairment in regeneration was further supported  
281 by a decreased level of expression of the proliferation marker *Pcna* in lung homogenate from NA-treated  
282 CARM1 deficient mice compared to WT controls ( $1.6 \pm 0.04$  vs  $1.9 \pm 0.1$ ,  $p < 0.05$ ) (Fig. 2F). Together,  
283 these results indicate that CARM1 is involved in the regenerative response to naphthalene-induced  
284 airway epithelial cell injury.

285

286 **CARM1 deficiency is not compensated by other closely related PRMT family members in mouse**  
287 **airway**

288 To exclude the possibility of compensation for the loss of CARM1 (Fig. 3A) by overexpression of other  
289 PRMTs, we examined the expression levels of the relevant PRMT family members PRMT1, PRMT5 and



290 PRMT7. CARM1 and PRMT1 can act in cooperation to enhance gene transcription (24) and both CARM1  
291 and PRMT5 have a role in the transcriptional regulation of cyclin E1 (12, 42). PRMT7 also functions in  
292 conjunction with PRMT5 (15). Our qRT-PCR data revealed no increase in the mRNA expression levels of  
293 these PRMTs in CARM1-deficient mouse lung compared to WT mice at day 14 following NA application  
294 (Fig. 3B-D).

295

### 296 **Contribution of CARM1 to airway epithelial senescence in mouse lung**

297 Club cell senescence plays an important role in the pathogenesis of COPD (2, 52). However, the  
298 underlying mechanism is not fully elucidated. We previously showed that CARM1 regulates alveolar  
299 epithelial senescence in an elastase-induced mouse model of emphysema (44). We thus hypothesized  
300 that CARM1 may also play an important role in the senescence of airway epithelial cells. We therefore  
301 performed immunohistochemical analysis for the anti-senescent protein SIRT1. This revealed a  
302 significantly reduced percentage of SIRT1-positive airway epithelial cells in *Carm1*<sup>+/-</sup> mice compared to  
303 WT controls at day 14 following NA application ( $73.5 \pm 3.3\%$  vs  $87.8 \pm 2\%$ ,  $p < 0.01$ ) (Fig. 4A, E). Next, we  
304 assessed lung sections for the senescence markers p21, p16 and beta-galactosidase activity. We  
305 observed that the basal level of airway epithelial cells positive for p21 (Fig. 4B, F) and p16 (Fig. 4C, G)  
306 were already significantly higher in *Carm1*<sup>+/-</sup> mice and the levels were not further increased by NA  
307 treatment. There was a significant increase in the number of beta-galactosidase positive cells in the  
308 airways of NA-treated *Carm1*<sup>+/-</sup> mice compared to NA-treated WT animals ( $31.8 \pm 3.4\%$  vs  $8.2 \pm 2.8\%$ ,  
309  $p < 0.001$ ) (Fig. 4D, H).

310 Moreover, western blot analysis of whole lung homogenates from d14 mice treated with NA revealed a  
311 clear reduction in the level of SIRT1 protein in *Carm1*<sup>+/-</sup> mice compared to WT controls (Fig. 5A, B), with a

312 concomitant increase in p53 levels (Fig. 5A, B). In addition, we analyzed the mRNA expression of *Sirt1*,  
313 *Cdkn1a* (p21) and *Cdkn2a* (p16) in whole lung homogenate. NA application downregulated *Sirt1* in WT  
314 mice but no change was observed in *Carm1*<sup>+/-</sup> mice (Fig. 5C). *Cdkn1a* was significantly increased in  
315 CARM1 deficient mice following NA treatment (Fig. 5D). For *Cdkn2a*, no changes in expression were  
316 detected (Fig. 5E). With respect to the differences in protein and mRNA expression levels, one has to  
317 take into account that the clear picture seen in the immunohistochemical analysis of a defined tissue,  
318 i.e. airway epithelium, is most likely obscured in the qPCR analysis of whole lung homogenate being  
319 dominated by tissues other than airway epithelium which, however, also express the genes analyzed. To  
320 confirm that the impaired regeneration of airway epithelial cells in *Carm1*<sup>+/-</sup> mice was a consequence of  
321 enhanced senescence in the club cells, dual immunofluorescence analysis for the anti-senescent protein  
322 SIRT1 or beta-galactosidase activity with CC10 was undertaken. Fig. 5F clearly reveals the presence of  
323 SIRT1 positive club cells at day 14 following NA application in WT mice, that is not detectable in *Carm1*<sup>+/-</sup>  
324 mice. Consistent with this, the few CC10 positive cells in the airways of *Carm1*<sup>+/-</sup> mice at day 14 following  
325 NA application are beta-galactosidase positive (Fig. 5G). Together, this data demonstrates that CARM1  
326 deficiency contributes to NA-induced airway epithelial cell injury by enhancing senescence in club cells,  
327 which is contributing to the impaired airway regeneration observed in *Carm1*<sup>+/-</sup> NA-treated mice.

328

### 329 **CARM1 regulates wound healing and senescence in human airway epithelial cells**

330 To translate our findings from the mouse model into humans, we examined the effects of a reduction of  
331 CARM1 in a human bronchial epithelial cell line (16HBE) following siRNA knock-down. The siRNA  
332 transfection significantly reduced *CARM1* mRNA expression by 72 ± 9.9% (Fig. 6A). We conducted a  
333 functional wound healing assay, where the siCARM1-transfected cell monolayer was scratched to induce

334 a wound. CARM1-silenced cells exhibited impaired wound healing compared with scrambled siRNA, as  
335 demonstrated by a larger wound area after 18h (Fig. 6B, C). To determine whether alterations in  
336 CARM1 expression regulates senescence in human bronchial epithelial cells, we analyzed the level of  
337 beta-galactosidase-positive cells. Consistent with mouse airway epithelial cells, the siCARM1-transfected  
338 human cells showed a significantly higher percentage of beta-galactosidase-positive cells compared with  
339 scrambled controls ( $13.2 \pm 0.6\%$  vs  $3.7 \pm 0.6\%$ ,  $p < 0.001$ ) (Fig. 6D, E). Mechanistically, CARM1-silenced  
340 cells demonstrated reduced expression of *SIRT1* (Fig. 6F), and treating CARM1-silenced cells with the  
341 SIRT1 activator resveratrol (39), reversed the impaired wound healing (Fig. 6G). In addition, blocking  
342 SIRT1 activity with the drug Ex-527 (14), impaired wound healing similar to that observed in CARM1-  
343 silenced cells (Fig. 6H). Thus, CARM1 reduction leads to cellular senescence in human airway epithelial  
344 cells. By undertaking gene set enrichment analysis (GSEA) upon publically available transcriptomics data  
345 of airway epithelial cells from COPD (n=22) versus healthy smoker (n=72) controls (GSE11784), we  
346 clearly identify airway epithelial cell senescence as a key component of COPD (Fig. 6I). Interestingly, we  
347 observe a clear reduction in the expression of *CARM1* in isolated bronchial epithelial cells from COPD  
348 patients compared to healthy smoking controls (Fig. 6J). Overall, this data implies that CARM1 regulates  
349 repair and regeneration in airway epithelial cells by affecting SIRT1 regulated cellular senescence.

350

## 351 **Discussion**

352 In physiological conditions, the airway epithelium has a rapid self-repair capacity following an insult that  
353 causes denudation of cells from the airway. However, repetitive exposure to cigarette smoke and/or  
354 other environmental particles can cause a chronic injury to the airway epithelium (11, 30). The injury can  
355 lead to altered migration, proliferation and re-differentiation processes which ultimately result in the  
356 airway remodeling observed in COPD pathogenesis (17). However, the underlying regulatory  
357 mechanisms of airway epithelial repair that are unique to COPD are still not well understood. Here, we  
358 investigated the function of the protein arginine methyltransferase CARM1 in airway epithelial repair.  
359 We demonstrated that CARM1 is expressed by CC10 positive club cells in both human and mouse  
360 airways and for the first time that it contributes to airway repair and regeneration by regulating airway  
361 epithelial cell senescence.

362 To simulate airway epithelial damage occurring in the lungs of patients with COPD, we used the widely  
363 accepted naphthalene (NA)-induced murine injury model. NA and several close structural analogs  
364 specifically target club cells, irrespective of the route of administration while alveolar epithelial type I or  
365 II cells remain uninjured in all animal species tested (7). Club cells, the progenitor cells in the airway  
366 epithelium, undergo cell death and exfoliation at 1–2 days following NA application (Fig. 1B-D) (9, 38)  
367 but are regenerated by d28 (Fig. 1B-D). The high susceptibility to NA is due to the high rate of metabolic  
368 activation leading to cytotoxicity catalyzed by the P450 monooxygenase CYP2F2 localized within the club  
369 cells (7). Interestingly, the loss in club cell number following injury was accompanied by a reduction in  
370 CARM1 expressing cells (Fig. 1E-G). Interestingly, a complete loss of CARM1 causes disrupted  
371 differentiation and proliferation of lung alveolar epithelial type-II cells (34). Previously, we showed that  
372 CARM1 contributes to ATII cell repair and regeneration by regulating cellular senescence (44). We  
373 therefore hypothesized that CARM1 plays a role in airway epithelial cell maintenance as well. Although

374 CARM1 is reported to be expressed in mouse club cells (34), here we additionally confirmed its  
375 expression in club cells of human airways. Club cells are nearly absent in the proximal airway epithelium  
376 of humans while 15% of proliferating airway epithelial cells in the terminal bronchioles are club cells (6).  
377 This reflects the significant role of club cells in the homeostasis of distal airways in humans. Therefore,  
378 we used the club cell targeted NA-induced injury model to understand the functional role of CARM1 in  
379 the airway repair process.

380 Airway epithelial cell damage is usually followed by proliferation that repairs the airway epithelium by  
381 day 10 after NA treatment and completes the reconstruction process by day 20 (22). We too, followed  
382 histological changes until day 28 following NA exposure, and observed a complete recovery of airway  
383 epithelium. The finding was corroborated by a significant downregulation of CARM1 expression in the  
384 airway and whole lung homogenate. CARM1 was previously reported to regulate the proliferation of  
385 neural cell lines (13). Loss of CARM1 has been linked to the developmental arrest in thymocyte  
386 progenitor cells due to dysfunctional differentiation (23). However, it is not known whether CARM1  
387 plays a role in the regeneration of airway epithelial cells. As mice with a complete knockout of CARM1  
388 cannot survive beyond late embryogenesis (34), we investigated the repair of airways in *Carm1*<sup>+/-</sup> mice  
389 following NA treatment. Heterozygous mice had significantly reduced *Carm1* mRNA expression in the  
390 lungs, which was not compensated by an increase in the expression of other PRMT family members (Fig.  
391 3). There are several reports of compensation by closely related PRMTs in other models. PRMT6 and  
392 PRMT7 levels were elevated in an attempt to compensate for PRMT1 loss in embryonic fibroblasts (10).  
393 *Carm1*<sup>+/-</sup> mice demonstrated impaired club cell regeneration following NA treatment accompanied by  
394 enhanced levels of senescent airway epithelial cells. Our results therefore further strengthen CARM1s  
395 role in maintaining cellular homeostasis by regulating cellular senescence which contributes to the  
396 airway repair and regeneration process.

397 The induction of epithelial cell senescence is an established mechanism impairing the repair process  
398 following airway injury (52). In COPD patients, senescence occurs in CC10-positive club cells (52).  
399 Chronic LPS exposure triggers senescence in airway epithelial cells evident by increased senescence  
400 associated beta galactosidase activity (43). Interestingly, CARM1 regulates cellular senescence. It is  
401 down-regulated in various organs including testis, thymus, and heart of aging rats (19). Senescent  
402 human diploid fibroblasts also expressed reduced levels of CARM1 (27). Mechanistically, CARM1  
403 represses senescence by methylating the RNA binding protein HuR, which regulates the turnover of  
404 SIRT1 mRNA (8, 36). SIRT1, a NAD<sup>+</sup>-dependent lysine deacetylase is known to suppress the senescence-  
405 associated secretome (16), and SIRT1 pathway dysregulation has been observed in smoke-exposed  
406 airway epithelium (3). Here we demonstrated that CARM1 deficiency led to lower levels of SIRT1  
407 positive airway epithelial cells after an insult by NA. In addition, we observed increased basal levels of  
408 p16 and p21 positive airway epithelial cells in CARM1 deficient mice which indicate an intrinsic pro-  
409 senescent status. CARM1-dependent methylation has been shown to regulate *Cdkn2a* (p16) mRNA by  
410 HuR-mediated stabilization (36). CARM1-dependent arginine methylation of HuD can also affect mRNA  
411 turnover of *Cdkn1a* (p21) (13). However, HuD mRNA is uniquely expressed in brain tissue but not the  
412 lungs. Therefore, in the lungs CARM1 might regulate *Cdkn1a* transcription by a different mechanism.  
413 CARM1 methylates the transcriptional coactivator p300, which is preferentially targeted by BRCA1 to  
414 induce expression of *Cdkn1a* (26). Further proof for CARM1-regulated cellular senescence in airway  
415 epithelial cells, was demonstrated by an increase in the number of beta galactosidase-positive airway  
416 epithelial cells in *Carm1*<sup>+/-</sup> mice compared to WT animals following NA treatment that localized to CC10  
417 positive cells.

418 In support of our findings with the mouse model and to translate this into human disease, we  
419 demonstrated by using human bronchial epithelial cells, that siRNA knock-down of CARM1 *in vitro* led to

420 reduced *SIRT1* expression, impaired wound healing and resulted in higher beta-galactosidase activity  
421 compared to scrambled-siRNA treated controls. *CARM1* reduction therefore leads to cellular senescence  
422 in human airway epithelial cells. The 16HBE cells used are not a model for club cells suggesting *CARM1*  
423 may have the potential to regulate senescence in other airway epithelial cell types. Our GSEA analysis of  
424 transcriptomics data from the airways of COPD patients compared to healthy smokers reiterates the  
425 contribution of airway senescence to COPD, and our own COPD data set confirms that this is  
426 accompanied by reduced *CARM1* expression. Taken together, our data implies that *CARM1* is necessary  
427 for the repair and regeneration of airway epithelial cells by regulating cellular senescence. Thus,  
428 highlighting the potential of *CARM1* as a novel therapeutic target in the treatment against airway injury  
429 observed in COPD patients.

430

431 **Acknowledgements**

432 The authors acknowledge the technical assistance of Christine Hollauer and Maximilian Pankla.

433

434 **Grants**

435 This work was supported in part by the Helmholtz Association and The German Center for Lung Research

436 (DZL).

437

438 **Disclosures**

439 The authors declare no conflict of interest.

440

441



442 **References**

- 443 1. Global Strategy for The Diagnosis, Management, And Prevention of Chronic Obstructive  
444 Pulmonary Disease [https://goldcopd.org/wp-content/uploads/2018/11/GOLD-2019-v1.7-FINAL-](https://goldcopd.org/wp-content/uploads/2018/11/GOLD-2019-v1.7-FINAL-14Nov2018-WMS.pdf)  
445 [14Nov2018-WMS.pdf](https://goldcopd.org/wp-content/uploads/2018/11/GOLD-2019-v1.7-FINAL-14Nov2018-WMS.pdf). [19.03, 2019].
- 446 2. **Bar-Shai A, Sagiv A, Alon R, and Krizhanovsky V.** The role of Clara cell senescence in the  
447 pathogenesis of COPD. *The European respiratory journal* 44: 3245, 2014.
- 448 3. **Beane J, Cheng L, Soldi R, Zhang X, Liu G, Anderlind C, Lenburg ME, Spira A, and Bild AH.** SIRT1  
449 pathway dysregulation in the smoke-exposed airway epithelium and lung tumor tissue. *Cancer research*  
450 72: 5702-5711, 2012.
- 451 4. **Bedford MT, and Clarke SG.** Protein arginine methylation in mammals: who, what, and why.  
452 *Molecular cell* 33: 1-13, 2009.
- 453 5. **Blanc RS, and Richard S.** Arginine Methylation: The Coming of Age. *Molecular cell* 65: 8-24,  
454 2017.
- 455 6. **Boers JE, Ambergen AW, and Thunnissen FB.** Number and proliferation of clara cells in normal  
456 human airway epithelium. *American journal of respiratory and critical care medicine* 159: 1585-1591,  
457 1999.
- 458 7. **Buckpitt A, Boland B, Isbell M, Morin D, Shultz M, Baldwin R, Chan K, Karlsson A, Lin C, Taff A,**  
459 **West J, Fanucchi M, Van Winkle L, and Plopper C.** Naphthalene-induced respiratory tract toxicity:  
460 metabolic mechanisms of toxicity. *Drug metabolism reviews* 34: 791-820, 2002.
- 461 8. **Calvanese V, Lara E, Suarez-Alvarez B, Abu Dawud R, Vazquez-Chantada M, Martinez-Chantar**  
462 **ML, Embade N, Lopez-Nieva P, Horrillo A, Hmadcha A, Soria B, Piazzolla D, Herranz D, Serrano M,**  
463 **Mato JM, Andrews PW, Lopez-Larrea C, Esteller M, and Fraga MF.** Sirtuin 1 regulation of developmental  
464 genes during differentiation of stem cells. *Proceedings of the National Academy of Sciences of the United*  
465 *States of America* 107: 13736-13741, 2010.
- 466 9. **Carvalho-Oliveira IM, Charro N, Aarbiou J, Buijs-Offerman RM, Wilke M, Schettgen T, Kraus T,**  
467 **Titulaer MK, Burgers P, Luider TM, Penque D, and Scholte BJ.** Proteomic analysis of naphthalene-  
468 induced airway epithelial injury and repair in a cystic fibrosis mouse model. *Journal of proteome*  
469 *research* 8: 3606-3616, 2009.
- 470 10. **Dhar S, Vemulapalli V, Patananan AN, Huang GL, Di Lorenzo A, Richard S, Comb MJ, Guo A,**  
471 **Clarke SG, and Bedford MT.** Loss of the major Type I arginine methyltransferase PRMT1 causes  
472 substrate scavenging by other PRMTs. *Scientific reports* 3: 1311, 2013.
- 473 11. **Duffney PF, McCarthy CE, Nogales A, Thatcher TH, Martinez-Sobrido L, Phipps RP, and Sime PJ.**  
474 Cigarette smoke dampens antiviral signaling in small airway epithelial cells by disrupting TLR3 cleavage.  
475 *American journal of physiology Lung cellular and molecular physiology* 314: L505-L513, 2018.
- 476 12. **El Messaoudi S, Fabbrizio E, Rodriguez C, Chuchana P, Fauquier L, Cheng D, Theillet C, Vandell**  
477 **L, Bedford MT, and Sardet C.** Coactivator-associated arginine methyltransferase 1 (CARM1) is a positive  
478 regulator of the Cyclin E1 gene. *Proceedings of the National Academy of Sciences of the United States of*  
479 *America* 103: 13351-13356, 2006.
- 480 13. **Fujiwara T, Mori Y, Chu DL, Koyama Y, Miyata S, Tanaka H, Yachi K, Kubo T, Yoshikawa H, and**  
481 **Tohyama M.** CARM1 regulates proliferation of PC12 cells by methylating HuD. *Molecular and cellular*  
482 *biology* 26: 2273-2285, 2006.
- 483 14. **Gertz M, Fischer F, Nguyen GT, Lakshminarasimhan M, Schutkowski M, Weyand M, and**  
484 **Steegborn C.** Ex-527 inhibits Sirtuins by exploiting their unique NAD<sup>+</sup>-dependent deacetylation  
485 mechanism. *Proceedings of the National Academy of Sciences of the United States of America* 110:  
486 E2772-2781, 2013.

- 487 15. **Gonsalvez GB, Tian L, Ospina JK, Boisvert FM, Lamond AI, and Matera AG.** Two distinct arginine  
488 methyltransferases are required for biogenesis of Sm-class ribonucleoproteins. *The Journal of cell*  
489 *biology* 178: 733-740, 2007.
- 490 16. **Hayakawa T, Iwai M, Aoki S, Takimoto K, Maruyama M, Maruyama W, and Motoyama N.**  
491 SIRT1 suppresses the senescence-associated secretory phenotype through epigenetic gene regulation.  
492 *PLoS one* 10: e0116480, 2015.
- 493 17. **Heijink IH, Brandenburg SM, Postma DS, and van Oosterhout AJ.** Cigarette smoke impairs  
494 airway epithelial barrier function and cell-cell contact recovery. *The European respiratory journal* 39:  
495 419-428, 2012.
- 496 18. **Hiemstra PS, McCray PB, Jr., and Bals R.** The innate immune function of airway epithelial cells in  
497 inflammatory lung disease. *The European respiratory journal* 45: 1150-1162, 2015.
- 498 19. **Hong E, Lim Y, Lee E, Oh M, and Kwon D.** Tissue-specific and age-dependent expression of  
499 protein arginine methyltransferases (PRMTs) in male rat tissues. *Biogerontology* 13: 329-336, 2012.
- 500 20. **Jia J, Conlon TM, Ballester Lopez C, Seimetz M, Bednorz M, Zhou-Suckow Z, Weissmann N,**  
501 **Eickelberg O, Mall MA, and Yildirim AO.** Cigarette smoke causes acute airway disease and exacerbates  
502 chronic obstructive lung disease in neonatal mice. *American journal of physiology Lung cellular and*  
503 *molecular physiology* 311: L602-610, 2016.
- 504 21. **John-Schuster G, Hager K, Conlon TM, Irmeler M, Beckers J, Eickelberg O, and Yildirim AO.**  
505 Cigarette smoke-induced iBALT mediates macrophage activation in a B cell-dependent manner in COPD.  
506 *American journal of physiology Lung cellular and molecular physiology* 307: L692-706, 2014.
- 507 22. **Karagiannis TC, Li X, Tang MM, Orlowski C, El-Osta A, Tang ML, and Royce SG.** Molecular model  
508 of naphthalene-induced DNA damage in the murine lung. *Human & experimental toxicology* 31: 42-50,  
509 2012.
- 510 23. **Kim J, Lee J, Yadav N, Wu Q, Carter C, Richard S, Richie E, and Bedford MT.** Loss of CARM1  
511 results in hypomethylation of thymocyte cyclic AMP-regulated phosphoprotein and deregulated early T  
512 cell development. *The Journal of biological chemistry* 279: 25339-25344, 2004.
- 513 24. **Kleinschmidt MA, Streubel G, Samans B, Krause M, and Bauer UM.** The protein arginine  
514 methyltransferases CARM1 and PRMT1 cooperate in gene regulation. *Nucleic acids research* 36: 3202-  
515 3213, 2008.
- 516 25. **Kuhn P, Chumanov R, Wang Y, Ge Y, Burgess RR, and Xu W.** Automethylation of CARM1 allows  
517 coupling of transcription and mRNA splicing. *Nucleic acids research* 39: 2717-2726, 2011.
- 518 26. **Lee YH, Bedford MT, and Stallcup MR.** Regulated recruitment of tumor suppressor BRCA1 to the  
519 p21 gene by coactivator methylation. *Genes & development* 25: 176-188, 2011.
- 520 27. **Lim Y, Lee E, Lee J, Oh S, and Kim S.** Down-regulation of asymmetric arginine methylation during  
521 replicative and H<sub>2</sub>O<sub>2</sub>-induced premature senescence in WI-38 human diploid fibroblasts. *J Biochem* 144:  
522 523-529, 2008.
- 523 28. **Lozano R, Naghavi M, Foreman K, Lim S, Shibuya K, Aboyans V, Abraham J, Adair T, Aggarwal**  
524 **R, Ahn SY, Alvarado M, Anderson HR, Anderson LM, Andrews KG, Atkinson C, Baddour LM, Barker-**  
525 **Collo S, Bartels DH, Bell ML, Benjamin EJ, Bennett D, Bhalla K, Bikbov B, Bin Abdulhak A, Birbeck G,**  
526 **Blyth F, Bolliger I, Boufous S, Bucello C, Burch M, Burney P, Carapetis J, Chen H, Chou D, Chugh SS,**  
527 **Coffeng LE, Colan SD, Colquhoun S, Colson KE, Condon J, Connor MD, Cooper LT, Corriere M, Cortinovis**  
528 **M, de Vaccaro KC, Couser W, Cowie BC, Criqui MH, Cross M, Dabhadkar KC, Dahodwala N, De Leo D,**  
529 **Degenhardt L, Delossantos A, Denenberg J, Des Jarlais DC, Dharmaratne SD, Dorsey ER, Driscoll T,**  
530 **Duber H, Ebel B, Erwin PJ, Espindola P, Ezzati M, Feigin V, Flaxman AD, Forouzanfar MH, Fowkes FG,**  
531 **Franklin R, Fransen M, Freeman MK, Gabriel SE, Gakidou E, Gaspari F, Gillum RF, Gonzalez-Medina D,**  
532 **Halasa YA, Haring D, Harrison JE, Havmoeller R, Hay RJ, Hoen B, Hotez PJ, Hoy D, Jacobsen KH, James**  
533 **SL, Jassrasaria R, Jayaraman S, Johns N, Karthikeyan G, Kassebaum N, Keren A, Khoo JP, Knowlton LM,**

534 **Kobusingye O, Koranteng A, Krishnamurthi R, Lipnick M, Lipshultz SE, Ohno SL, Mabweijano J,**  
535 **MacIntyre MF, Mallinger L, March L, Marks GB, Marks R, Matsumori A, Matzopoulos R, Mayosi BM,**  
536 **McAnulty JH, McDermott MM, McGrath J, Mensah GA, Merriman TR, Michaud C, Miller M, Miller TR,**  
537 **Mock C, Mocumbi AO, Mokdad AA, Moran A, Mulholland K, Nair MN, Naldi L, Narayan KM, Nasser K,**  
538 **Norman P, O'Donnell M, Omer SB, Ortblad K, Osborne R, Ozgediz D, Pahari B, Pandian JD, Rivero AP,**  
539 **Padilla RP, Perez-Ruiz F, Perico N, Phillips D, Pierce K, Pope CA, 3rd, Porrini E, Pourmalek F, Raju M,**  
540 **Ranganathan D, Rehm JT, Rein DB, Remuzzi G, Rivara FP, Roberts T, De Leon FR, Rosenfeld LC, Rushton**  
541 **L, Sacco RL, Salomon JA, Sampson U, Sanman E, Schwebel DC, Segui-Gomez M, Shepard DS, Singh D,**  
542 **Singleton J, Sliwa K, Smith E, Steer A, Taylor JA, Thomas B, Tleyjeh IM, Towbin JA, Truelsen T,**  
543 **Undurraga EA, Venketasubramanian N, Vijayakumar L, Vos T, Wagner GR, Wang M, Wang W, Watt K,**  
544 **Weinstock MA, Weintraub R, Wilkinson JD, Woolf AD, Wulf S, Yeh PH, Yip P, Zabetian A, Zheng ZJ,**  
545 **Lopez AD, Murray CJ, AlMazroa MA, and Memish ZA.** Global and regional mortality from 235 causes of  
546 death for 20 age groups in 1990 and 2010: a systematic analysis for the Global Burden of Disease Study  
547 2010. *Lancet* 380: 2095-2128, 2012.

548 29. **May SM, and Li JT.** Burden of chronic obstructive pulmonary disease: healthcare costs and  
549 beyond. *Allergy and asthma proceedings* 36: 4-10, 2015.

550 30. **McCarthy CE, Duffney PF, Gelein R, Thatcher TH, Elder A, Phipps RP, and Sime PJ.** Dung  
551 biomass smoke activates inflammatory signaling pathways in human small airway epithelial cells.  
552 *American journal of physiology Lung cellular and molecular physiology* 311: L1222-L1233, 2016.

553 31. **McDonough JE, Yuan R, Suzuki M, Seyednejad N, Elliott WM, Sanchez PG, Wright AC, Gefter**  
554 **WB, Litzky L, Coxson HO, Pare PD, Sin DD, Pierce RA, Woods JC, McWilliams AM, Mayo JR, Lam SC,**  
555 **Cooper JD, and Hogg JC.** Small-airway obstruction and emphysema in chronic obstructive pulmonary  
556 disease. *The New England journal of medicine* 365: 1567-1575, 2011.

557 32. **Meyer KF, Krauss-Etschmann S, Kooistra W, Reinders-Luinge M, Timens W, Kobzik L, Plosch T,**  
558 **and Hylkema MN.** Prenatal exposure to tobacco smoke sex dependently influences methylation and  
559 mRNA levels of the Igf axis in lungs of mouse offspring. *American journal of physiology Lung cellular and*  
560 *molecular physiology* 312: L542-L555, 2017.

561 33. **Mootha VK, Lindgren CM, Eriksson KF, Subramanian A, Sihag S, Lehar J, Puigserver P, Carlsson**  
562 **E, Ridderstrale M, Laurila E, Houstis N, Daly MJ, Patterson N, Mesirov JP, Golub TR, Tamayo P,**  
563 **Spiegelman B, Lander ES, Hirschhorn JN, Altshuler D, and Groop LC.** PGC-1alpha-responsive genes  
564 involved in oxidative phosphorylation are coordinately downregulated in human diabetes. *Nature*  
565 *genetics* 34: 267-273, 2003.

566 34. **O'Brien KB, Alberich-Jorda M, Yadav N, Kocher O, Diruscio A, Ebralidze A, Levantini E, Sng NJ,**  
567 **Bhasin M, Caron T, Kim D, Steidl U, Huang G, Halmos B, Rodig SJ, Bedford MT, Tenen DG, and**  
568 **Kobayashi S.** CARM1 is required for proper control of proliferation and differentiation of pulmonary  
569 epithelial cells. *Development* 137: 2147-2156, 2010.

570 35. **Ohkura N, Takahashi M, Yaguchi H, Nagamura Y, and Tsukada T.** Coactivator-associated  
571 arginine methyltransferase 1, CARM1, affects pre-mRNA splicing in an isoform-specific manner. *The*  
572 *Journal of biological chemistry* 280: 28927-28935, 2005.

573 36. **Pang L, Tian H, Chang N, Yi J, Xue L, Jiang B, Gorospe M, Zhang X, and Wang W.** Loss of CARM1  
574 is linked to reduced HuR function in replicative senescence. *BMC Mol Biol* 14: 15, 2013.

575 37. **Parikh P, Wicher S, Khandalavala K, Pabelick CM, Britt RD, Jr., and Prakash YS.** Cellular  
576 senescence in the lung across the age spectrum. *American journal of physiology Lung cellular and*  
577 *molecular physiology* 316: L826-L842, 2019.

578 38. **Plopper CG, Van Winkle LS, Fanucchi MV, Malburg SR, Nishio SJ, Chang A, and Buckpitt AR.**  
579 Early events in naphthalene-induced acute Clara cell toxicity. II. Comparison of glutathione depletion

580 and histopathology by airway location. *American journal of respiratory cell and molecular biology* 24:  
581 272-281, 2001.

582 39. **Price NL, Gomes AP, Ling AJ, Duarte FV, Martin-Montalvo A, North BJ, Agarwal B, Ye L,**  
583 **Ramadori G, Teodoro JS, Hubbard BP, Varela AT, Davis JG, Varamini B, Hafner A, Moaddel R, Rolo AP,**  
584 **Coppari R, Palmeira CM, de Cabo R, Baur JA, and Sinclair DA.** SIRT1 is required for AMPK activation and  
585 the beneficial effects of resveratrol on mitochondrial function. *Cell metabolism* 15: 675-690, 2012.

586 40. **Rackley CR, and Stripp BR.** Building and maintaining the epithelium of the lung. *The Journal of*  
587 *clinical investigation* 122: 2724-2730, 2012.

588 41. **Rawlins EL, Okubo T, Xue Y, Brass DM, Auten RL, Hasegawa H, Wang F, and Hogan BL.** The role  
589 of Scgb1a1+ Clara cells in the long-term maintenance and repair of lung airway, but not alveolar,  
590 epithelium. *Cell stem cell* 4: 525-534, 2009.

591 42. **Richard S, Morel M, and Cleroux P.** Arginine methylation regulates IL-2 gene expression: a role  
592 for protein arginine methyltransferase 5 (PRMT5). *The Biochemical journal* 388: 379-386, 2005.

593 43. **Sagiv A, Bar-Shai A, Levi N, Hatzav M, Zada L, Ovadya Y, Roitman L, Manella G, Regev O,**  
594 **Majewska J, Vadai E, Eilam R, Feigelson SW, Tsoory M, Tauc M, Alon R, and Krizhanovsky V.** p53 in  
595 Bronchial Club Cells Facilitates Chronic Lung Inflammation by Promoting Senescence. *Cell reports* 22:  
596 3468-3479, 2018.

597 44. **Sarker RS, John-Schuster G, Bohla A, Mutze K, Burgstaller G, Bedford MT, Konigshoff M,**  
598 **Eickelberg O, and Yildirim AO.** Coactivator-Associated Arginine Methyltransferase-1 Function in Alveolar  
599 Epithelial Senescence and Elastase-Induced Emphysema Susceptibility. *American journal of respiratory*  
600 *cell and molecular biology* 53: 769-781, 2015.

601 45. **Schamberger AC, Mise N, Meiners S, and Eickelberg O.** Epigenetic mechanisms in COPD:  
602 implications for pathogenesis and drug discovery. *Expert opinion on drug discovery* 9: 609-628, 2014.

603 46. **Shin HJ, Kim H, Oh S, Lee JG, Kee M, Ko HJ, Kweon MN, Won KJ, and Baek SH.** AMPK-SKP2-  
604 CARM1 signalling cascade in transcriptional regulation of autophagy. *Nature* 534: 553-557, 2016.

605 47. **Streubel G, Bouchard C, Berberich H, Zeller MS, Teichmann S, Adamkiewicz J, Muller R,**  
606 **Klempnauer KH, and Bauer UM.** PRMT4 is a novel coactivator of c-Myb-dependent transcription in  
607 haematopoietic cell lines. *PLoS genetics* 9: e1003343, 2013.

608 48. **Subramanian A, Tamayo P, Mootha VK, Mukherjee S, Ebert BL, Gillette MA, Paulovich A,**  
609 **Pomeroy SL, Golub TR, Lander ES, and Mesirov JP.** Gene set enrichment analysis: a knowledge-based  
610 approach for interpreting genome-wide expression profiles. *Proceedings of the National Academy of*  
611 *Sciences of the United States of America* 102: 15545-15550, 2005.

612 49. **Sundar IK, and Rahman I.** Gene expression profiling of epigenetic chromatin modification  
613 enzymes and histone marks by cigarette smoke: implications for COPD and lung cancer. *American*  
614 *journal of physiology Lung cellular and molecular physiology* 311: L1245-L1258, 2016.

615 50. **Vogelmeier CF, Criner GJ, Martinez FJ, Anzueto A, Barnes PJ, Bourbeau J, Celli BR, Chen R,**  
616 **Decramer M, Fabbri LM, Frith P, Halpin DM, Lopez Varela MV, Nishimura M, Roche N, Rodriguez-**  
617 **Roisin R, Sin DD, Singh D, Stockley R, Vestbo J, Wedzicha JA, and Agusti A.** Global Strategy for the  
618 Diagnosis, Management, and Prevention of Chronic Obstructive Lung Disease 2017 Report. GOLD  
619 Executive Summary. *American journal of respiratory and critical care medicine* 195: 557-582, 2017.

620 51. **Yildirim AO, Veith M, Rausch T, Muller B, Kilb P, Van Winkle LS, and Fehrenbach H.**  
621 Keratinocyte growth factor protects against Clara cell injury induced by naphthalene. *The European*  
622 *respiratory journal* 32: 694-704, 2008.

623 52. **Zhou F, Onizawa S, Nagai A, and Aoshiba K.** Epithelial cell senescence impairs repair process  
624 and exacerbates inflammation after airway injury. *Respiratory research* 12: 78, 2011.

625

626

627

628 **Figure legends**

629 **Figure 1. Naphthalene-induced bronchial epithelial injury down regulates CARM1 expression. (A)**

630 Representative immunofluorescence images of CC10 (Red) and CARM1 (Green) co-localization in airway  
631 epithelial cells of human lung sections (upper panel, representative of 4 lungs) and mouse lung sections  
632 (lower panel, representative of 4 lungs). Counterstained with DAPI (blue). **(B)** Airway-specific injury was  
633 induced in wild type C57BL/6 mice by intraperitoneal (i.p.) application of naphthalene (NA) dissolved in  
634 corn oil (CO) at a concentration of 200 mg/kg body weight. Control mice were treated with CO only.  
635 Representative immunohistochemical analysis of lung at the time points indicated, stained to detect  
636 CC10 (red) and haematoxylin counter stained. **(C)** Quantification of CC10 positive club cells by  
637 stereological analysis of lung sections described in B. **(D)** mRNA expression level of *Scgb1a1* (CC10) in  
638 mouse lung homogenate by qRT-PCR. **(E)** Representative immunohistochemical analysis of lung at the  
639 time points indicated from mice described in B, stained to detect CARM1 (red) and haematoxylin  
640 counter stained. **(F)** Quantification of CARM1 positive cells in the airways by stereological analysis of  
641 lung sections described in E. **(G)** mRNA expression level of *Carm1* in mouse lung homogenate by qRT-  
642 PCR. \*P<0.05, \*\*P<0.01, \*\*\*P<0.001, 1-way ANOVA followed by Bonferroni's multiple comparison post-  
643 test, CO vs NA-treated animals. Data presented are mean ± s.d. The experiments were repeated twice  
644 with 4-6 mice/group in each experiment.

645

646 **Figure 2. CARM1 deficiency impairs club cell regeneration following naphthalene-induced airway**

647 **injury.** Wild type (WT) or *Carm1*<sup>+/-</sup> mice treated with naphthalene (NA) or corn oil (CO) were assessed up  
648 to day 14 for body weight analysis or on day 14 for all other analyses. **(A)** Western blot analysis of

649 CARM1 expression in the lungs of WT and *Carm1*<sup>+/-</sup> mice following NA treatment. Expression relative to  
650  $\beta$ -actin shown, with each point indicating an individual mouse. (B) Western blot analysis of  
651 asymmetrically dimethylated arginine (ADMA) residues in protein isolated from the lungs of WT and  
652 *Carm1*<sup>+/-</sup> mice following NA treatment. Global expression relative to  $\beta$ -actin shown, with each point  
653 indicating an individual mouse. (C) Comparison of body weight between the mice described at the  
654 indicated time points. (D) Representative immunohistochemical analysis of lung stained to detect CC10  
655 (arrows indicate positively stained red cells) and haematoxylin counter stained. (E) Stereological  
656 quantification of CC10 positive club cells from lung sections described in B. (F) mRNA expression level of  
657 *Pcna* in mouse lung homogenate by qRT-PCR. \*P<0.05, \*\*P<0.01 and \*\*\*P<0.001, 1-way ANOVA  
658 followed by Bonferroni's multiple comparison post-test (E and F) and two-tailed unpaired t-test between  
659 NA *Carm1*<sup>+/-</sup> and NA WT mice (A-C). Data presented are mean  $\pm$  s.d. The experiments were repeated  
660 twice with 4-7 mice/group in each experiment.

661

662 **Figure 3. CARM1 deficiency is not compensated for by other closely related PRMT family members.**  
663 mRNA expression levels of *Carm1* (A), *Prmt1* (B), *Prmt5* (C) and *Prmt7* (D) in lung homogenate by qRT-  
664 PCR from wild type (WT) and *Carm1*<sup>+/-</sup> mice on day 14 post naphthalene (NA) or corn oil (CO) treatment.  
665 \*P<0.05, 1-way ANOVA followed by Bonferroni's multiple comparison post-test. Data presented are  
666 mean  $\pm$  s.d., from 4-7 mice/group.

667

668 **Figure 4. CARM1 deficiency leads to airway epithelial cell senescence in mouse lung following**  
669 **naphthalene treatment.** Wild type (WT) or *Carm1*<sup>+/-</sup> mice were treated with naphthalene (NA) or corn  
670 oil (CO) and analyzed on day 14. Representative immunohistochemical analysis of lung stained to detect

671 SIRT1 (A), p21 (B), p16 (C) and beta galactosidase (D), arrows indicate positively stained red cells.  
672 Haematoxylin counter stained. Stereological quantification of SIRT1 (E), p21 (F), p16 (G) and beta  
673 galactosidase (H) positive airway epithelial cells. \*P<0.05, \*\*P<0.01, \*\*\*P<0.001, 1-way ANOVA followed  
674 by Bonferroni's multiple comparison post-test. Data presented are mean  $\pm$  s.d., from 4-7 mice/group.

675

676 **Figure 5. Club cell senescence in the airways of *Carm1*<sup>+/-</sup> mice following naphthalene treatment.** Wild  
677 type (WT) or *Carm1*<sup>+/-</sup> mice were treated with naphthalene (NA) or corn oil (CO) and analyzed on day 14.  
678 (A) Western blot analysis of SIRT1 and p53 expression in the lungs of WT and *Carm1*<sup>+/-</sup> mice following NA  
679 treatment. (B) SIRT1 and p53 expression relative to  $\beta$ -actin taken from (A), with each point indicating an  
680 individual mouse. \*P<0.05, two-tailed unpaired t-test. mRNA expression levels of *Sirt1* (C), *Cdkn1a* (p21)  
681 (D) and *Cdkn2a* (p16) (E) in mouse lung homogenate by qRT-PCR. \*P<0.05 1-way ANOVA followed by  
682 Bonferroni's multiple comparison post-test. Data presented are mean  $\pm$  s.d., from 4-7 mice/group. (F)  
683 Representative immunofluorescence analysis of lung stained to detect SIRT1 (Red) and CC10 (Green),  
684 counterstained with DAPI (blue). White arrows highlight CC10 positive cells lacking SIRT1 expression. (G)  
685 Representative immunofluorescence analysis of lung stained to detect beta galactosidase (Red) and  
686 CC10 (Green), counterstained with DAPI (blue). White arrows indicate CC10 and beta galactosidase  
687 double positive cells. Images representative of 4 mice per group.

688

689 **Figure 6. CARM1 promotes repair and regeneration of human bronchial epithelial cells by regulating**  
690 **senescence.** 16HBE cells were transfected with a cocktail of CARM1 specific siRNAs (siCARM1) or non-  
691 specific scrambled siRNA (Sc) for 72 hours. Untreated cells were taken as medium control (CO). (A)  
692 mRNA expression level of *CARM1* by qRT-PCR. (B) Wound healing assay was performed by scratching

693 confluent siRNA-transfected 16HBE cell monolayers, wound size was determined 18 h after injury and  
694 reported as percentage closure. (C) Representative images of wound size at time 0 h and 18 h. (D)  
695 siRNA-transfected 16HBE cells were incubated overnight with beta galactosidase staining solution and  
696 the number of positive cells quantified. (E) Representative images from the assay in D. (F) mRNA  
697 expression level of *SIRT1* by qRT-PCR. (G) siCARM1 cells were additionally treated with 1 $\mu$ M Resveratrol  
698 24h before performing the scratch and wound size determined 18h after injury and reported as  
699 percentage closure. (H) 16HBE cells were treated with Ex-527 at the concentrations shown for 24h prior  
700 to performing a scratch assay, and wound size determined 18h after injury and reported as percentage  
701 closure. (I) Gene set enrichment analysis (GSEA) of cell senescence genes (GO: 0090398) in publically  
702 available array data from the small airways of COPD patients (n=22) v healthy smokers (n=72)  
703 (GSE11784), the normalized enrichment score (NES), P value and false discovery rate (FDR) are also  
704 indicated. (J) mRNA expression level of *CARM1* by qRT-PCR in isolated bronchial epithelial cells from  
705 COPD patients (n=8) compared to healthy smoking controls (n=10). Data presented (A-H) are mean  $\pm$   
706 s.d., representative of three independent experiments with n=2/3 per group in each experiment.  
707 \*P<0.05, \*\*P<0.01, \*\*\*P<0.001 student's two-tailed t-test.

708



	<b>Smokers</b>	<b>COPD</b>
<b>Subjects (n)</b>	10	8
<b>Female/Male</b>	4/6	0/8
<b>Mean age years</b>	61.5 ± 3.93	65.25 ± 3.21
<b>Smoking (packs/year)</b>	38.75 ± 13.11	44.00 ± 4.58
<b>FEV1 (%)</b>	103.8 ± 5.44	94.88 ± 3.93
<b>FVC (%)</b>	102.1 ± 5.63	75.88 ± 4.47 *
<b>FEV1/FVC (%)</b>	80.35 ± 1.98	62.31 ± 2.86 **
<b>GOLD (mean, min-max)</b>	NA	2 (2,2)

710 **FEV1:** Forced expiratory volume in the first second; **FVC:** Forced vital capacity.

711 \*: p<0.01, \*\*: p<0.001 COPD versus smokers.

712

713 **Table 1.** Clinical characteristics and demographics of subjects for the primary bronchial epithelial cell

714 cultures (Mean ± SEM).

715

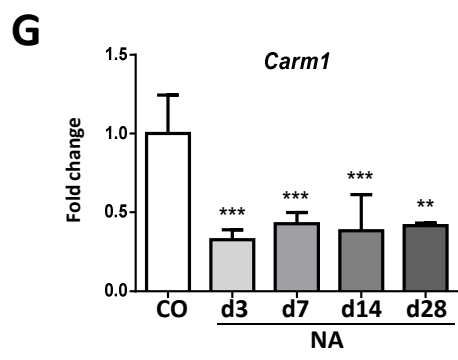
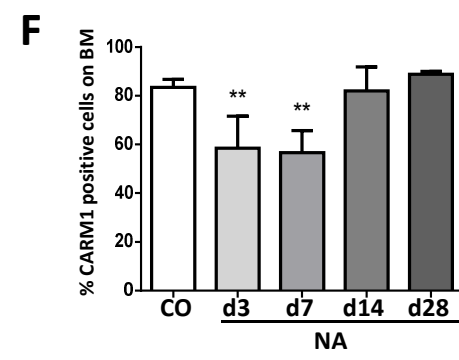
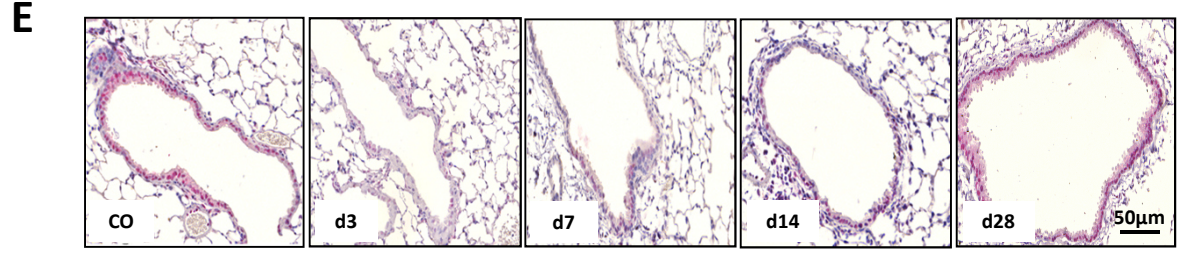
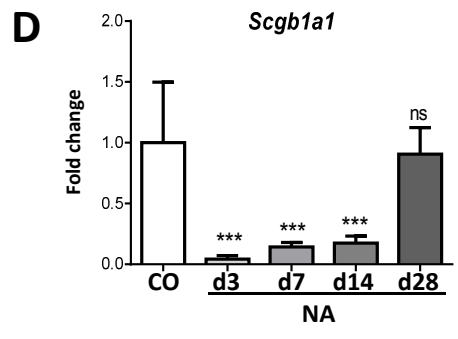
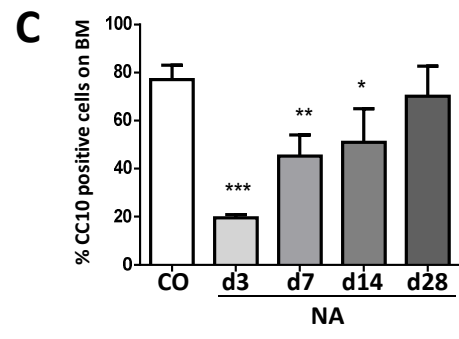
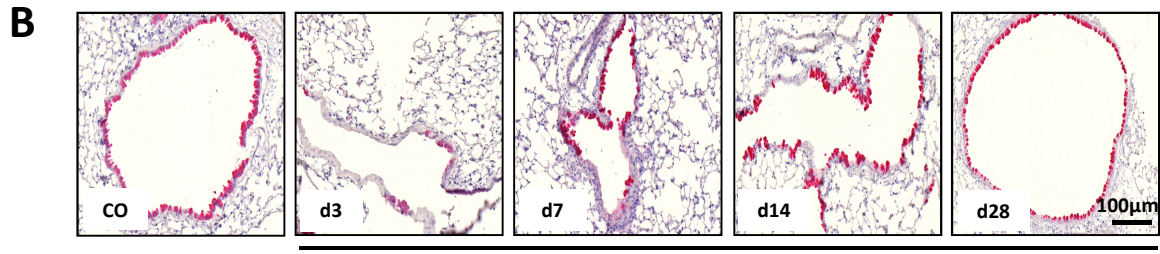
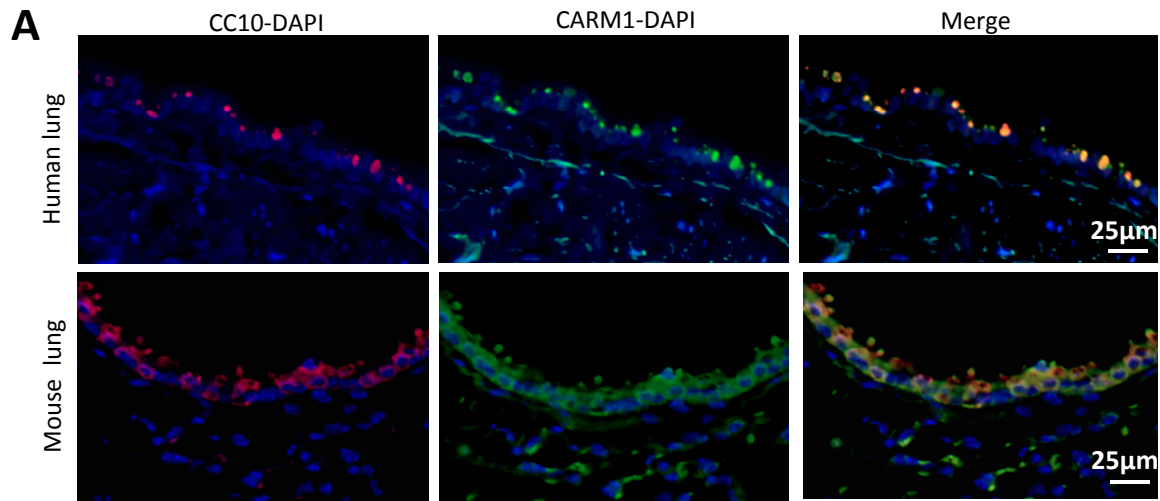
716

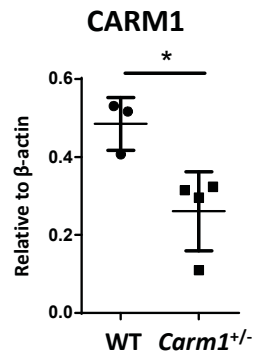
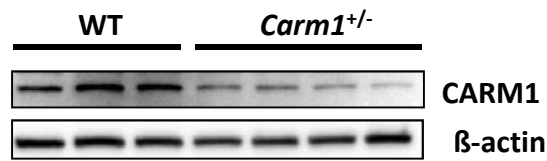
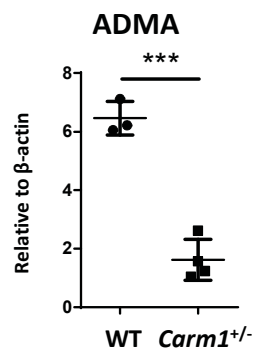
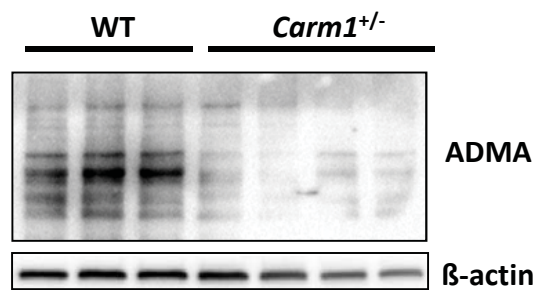
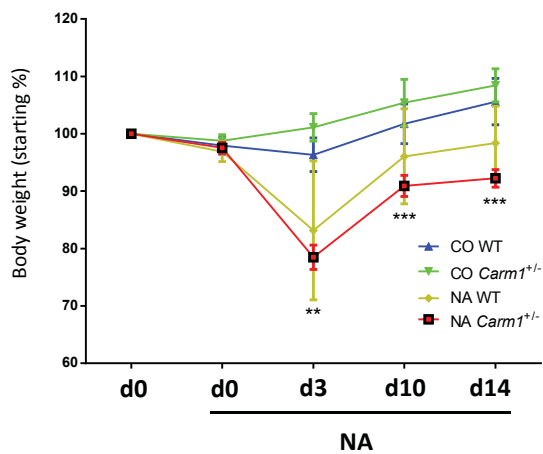
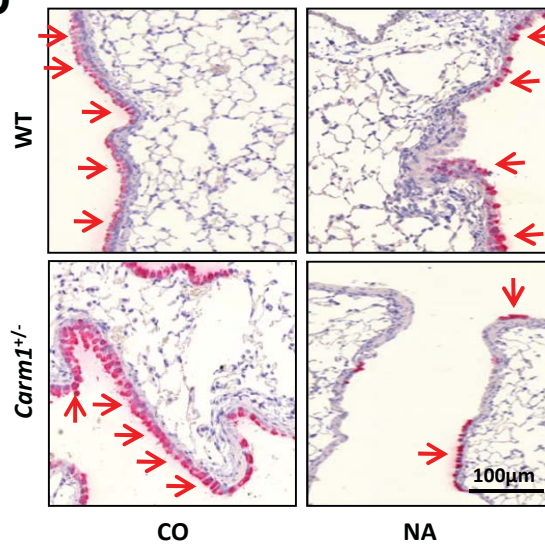
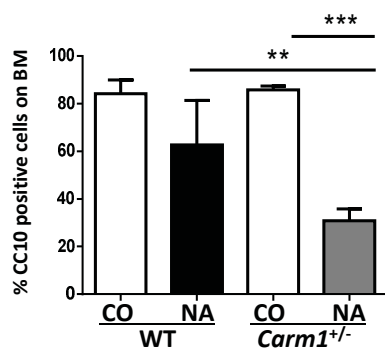
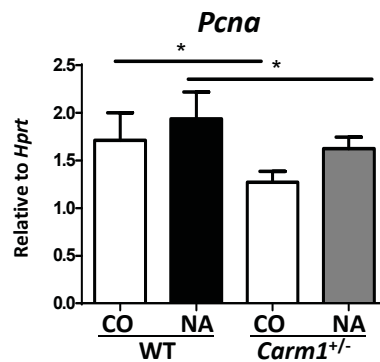
717

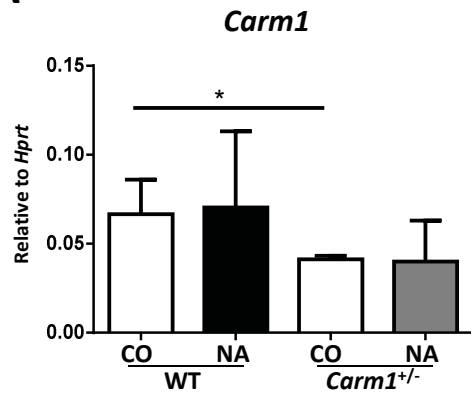
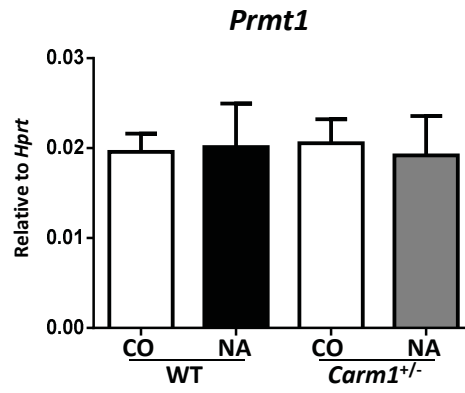
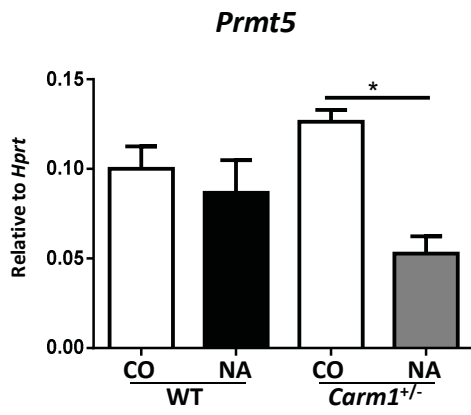
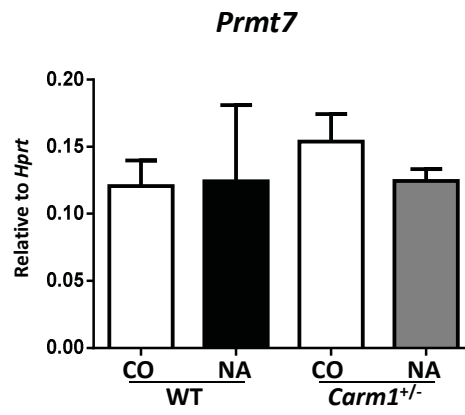
Gene	Forward primer	Reverse primer
<i>Carm1</i>	GTGGGCAGACAGTCCTTCAT	GTCCGCTCACTGAACACAGA
<i>Cdkn1a</i>	CGGTGTCAGAGTCTAGGGGA	AGAGACAACGGCACACTTTG
<i>Cdkn2a</i>	TCGTGAACATGTTGTTGAGGC	CTACGTGAACGTTGCCATC
<i>Hprt1</i>	CCTAAGATGAGCGCAAGTTGAA	CCACAGGACTAGAACACCTGCTAA
<i>Pcna</i>	CCACATTGGAGATGCTGTTG	CCGCCTCCTCTTCTTTATCC
<i>Prmt1</i>	CGAACTGCATCATGGAGAAT	AGCGTTGGGCTTCTCCACTAC
<i>Prmt5</i>	TGACCAACCACATCCCACT	GTGTGTAGTCGGGGCATTCT
<i>Prmt7</i>	TACTGCAGGGGCTGACTTCT	TCACCTCAGTGGAGTGCTTG
<i>Scgb1a1</i>	ACCTCTACCATGAAGATCGCC	CTCTGATTCCATGAGGAGGGC
<i>Sirt1</i>	CCATTAATGAGGAAAGCAATAGGC	AATACAAGGCTAACACCTTGGG
<i>CARM1</i>	ACAGCGTCCTCAATCCAGTTC	GCTGGGACAGGTAGGCATAA
<i>SIRT1</i>	GCAGATTAGTAGGCGGCTTG	TCTGGCATGTCCCACTATCA
<i>GAPDH</i>	ATGGAAATCCCATCACCATCTT	CGCCCCACTTGATTTTGG

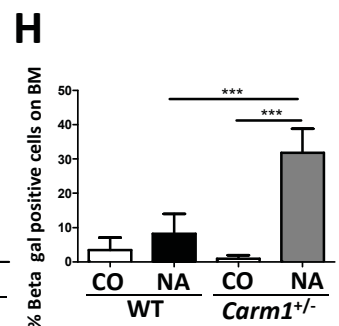
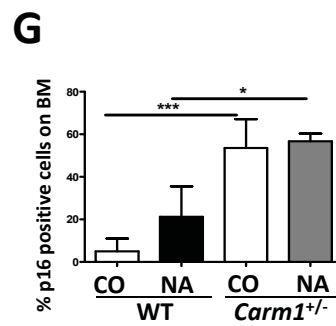
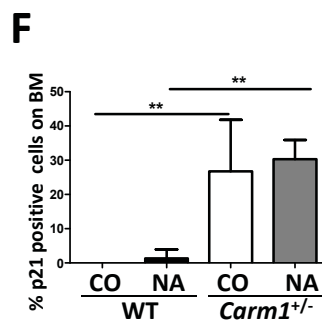
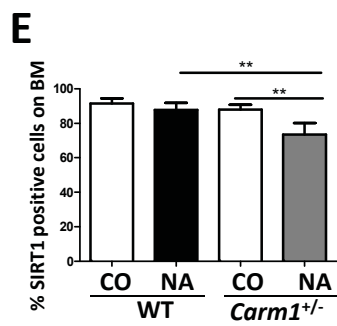
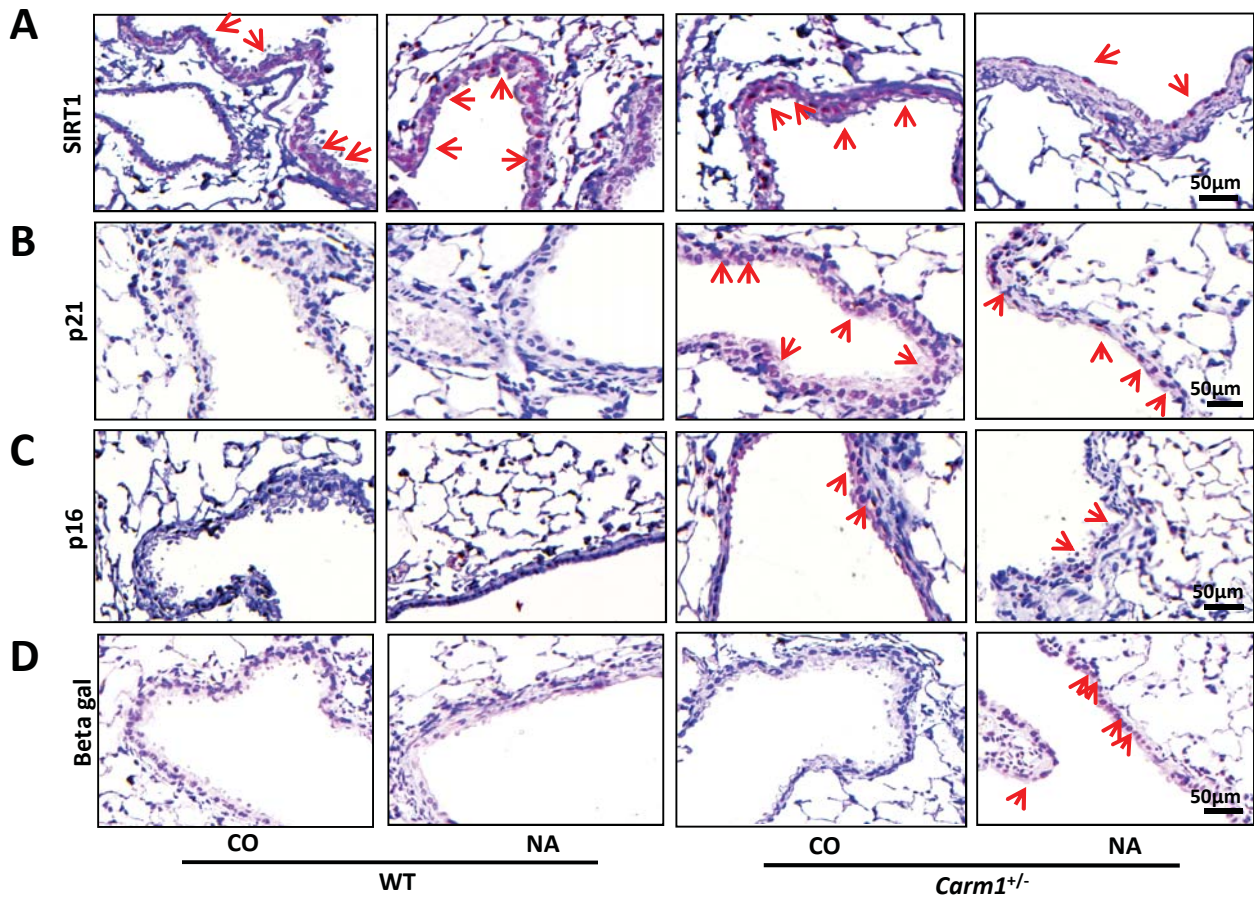
718

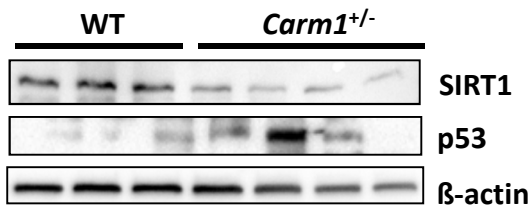
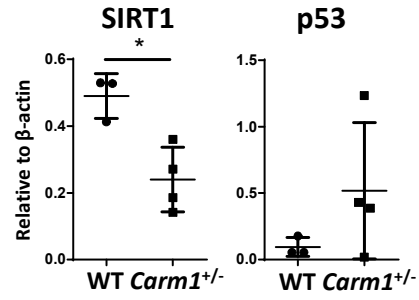
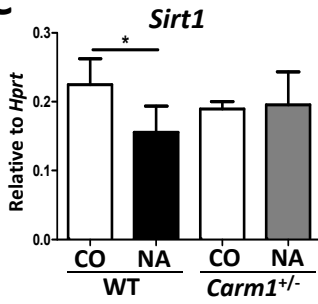
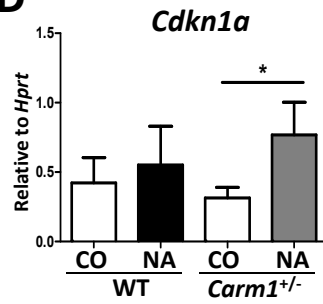
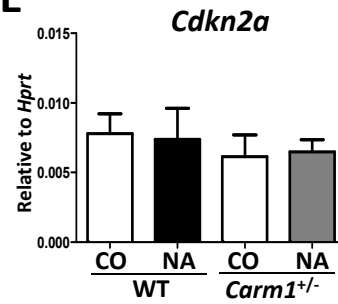
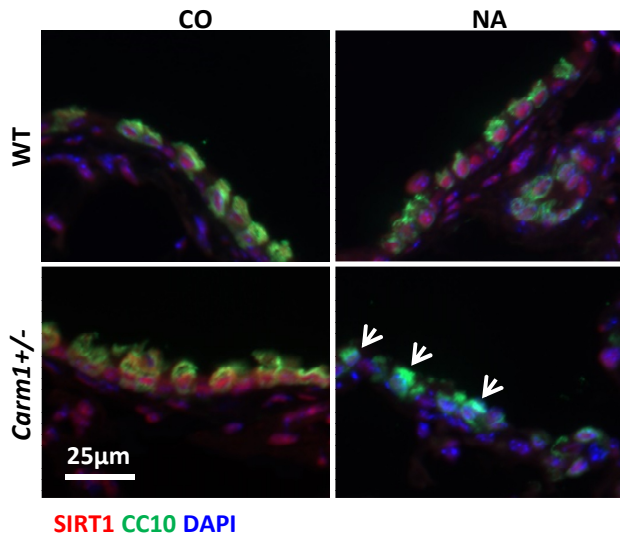
719 **Table 2.** Primers used for quantitative real time PCR.



**A****B****C****D****E****F**

**A****B****C****D**



**A****B****C****D****E****F****G**